Article

Developmental Cell

Nerves Regulate Cardiomyocyte Proliferation and Heart Regeneration

Graphical Abstract

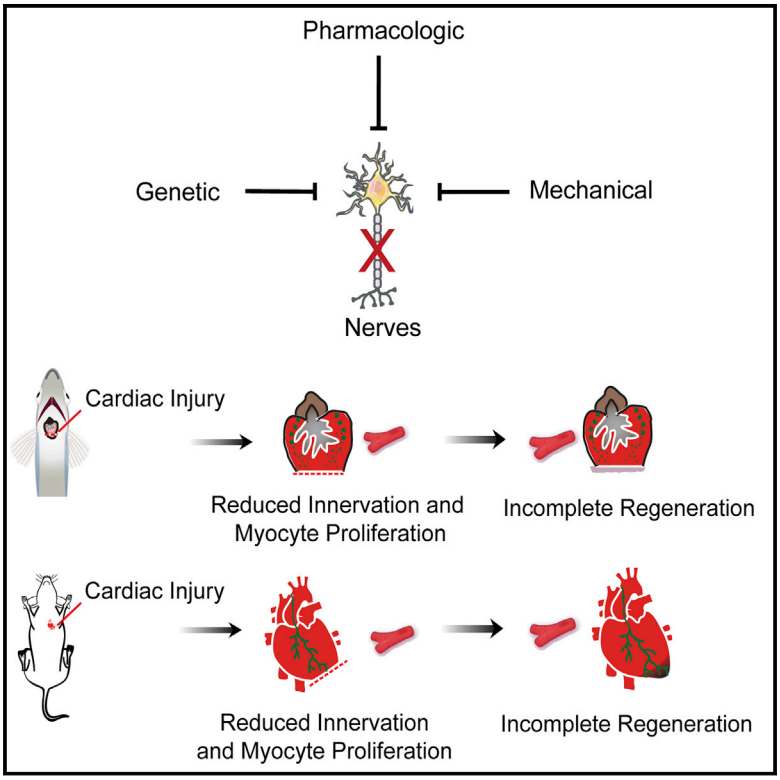

Authors

Ahmed I. Mahmoud, Caitlin C. O'Meara, Matthew Gemberling, ..., Calum A. MacRae, Kenneth D. Poss, Richard T. Lee

Correspondence

rlee@partners.org

In Brief

Mahmoud et al. demonstrate that nerves are required for cardiomyocyte proliferation during both zebrafish and neonatal mouse heart regeneration. The negative effect of hypoinnervation on regeneration can be partially rescued by NRG1 and NGF proteins.

Highlights

- Hypo-innervation of the zebrafish heart impairs heart regeneration
- Cholinergic signaling guides myocyte proliferation in zebrafish and neonatal mice
- Neonatal mouse vagotomy impairs myocyte proliferation and heart regeneration
- Neonatal vagotomy reduces the inflammatory response following heart injury

Accession Numbers

GSE69855
GSE69775

Mahmoud et al., 2015, Developmental Cell *34*, 387–399
August 24, 2015
http://dx.doi.org/10.1016/j.devcel.2015.06.017

Developmental Cell
Article

Nerves Regulate Cardiomyocyte Proliferation and Heart Regeneration

Ahmed I. Mahmoud,[1,2,4,6] Caitlin C. O'Meara,[1,2,4,6] Matthew Gemberling,[5] Long Zhao,[2,3] Donald M. Bryant,[1,2,4] Ruimao Zheng,[1,2,4] Joseph B. Gannon,[1,2,4] Lei Cai,[1,2,4] Wen-Yee Choi,[5] Gregory F. Egnaczyk,[5] Caroline E. Burns,[2,3] C. Geoffrey Burns,[2,3] Calum A. MacRae,[2,4] Kenneth D. Poss,[5] and Richard T. Lee[1,2,4,*]

[1]Department of Stem Cell and Regenerative Biology, Harvard University, and the Brigham Regenerative Medicine Center, Brigham and Women's Hospital and Harvard Medical School, Cambridge, MA 02139, USA
[2]Harvard Stem Cell Institute, Cambridge, MA 02138, USA
[3]Department of Medicine, Cardiovascular Research Center, Massachusetts General Hospital and Harvard Medical School, Charlestown, MA 02129, USA
[4]Department of Medicine, Cardiovascular Division, Brigham and Women's Hospital and Harvard Medical School, Boston, MA 02115, USA
[5]Department of Cell Biology and Howard Hughes Medical Institute, Duke University Medical Center, Durham, NC 27710, USA
[6]Co-first author
*Correspondence: rlee@partners.org
http://dx.doi.org/10.1016/j.devcel.2015.06.017

SUMMARY

Some organisms, such as adult zebrafish and newborn mice, have the capacity to regenerate heart tissue following injury. Unraveling the mechanisms of heart regeneration is fundamental to understanding why regeneration fails in adult humans. Numerous studies have revealed that nerves are crucial for organ regeneration, thus we aimed to determine whether nerves guide heart regeneration. Here, we show using transgenic zebrafish that inhibition of cardiac innervation leads to reduction of myocyte proliferation following injury. Specifically, pharmacological inhibition of cholinergic nerve function reduces cardiomyocyte proliferation in the injured hearts of both zebrafish and neonatal mice. Direct mechanical denervation impairs heart regeneration in neonatal mice, which was rescued by the administration of neuregulin 1 (NRG1) and nerve growth factor (NGF) recombinant proteins. Transcriptional analysis of mechanically denervated hearts revealed a blunted inflammatory and immune response following injury. These findings demonstrate that nerve function is required for both zebrafish and mouse heart regeneration.

INTRODUCTION

A significant cause of heart failure is the inability of the adult mammalian heart to replace lost cells following injury (Laflamme and Murry, 2011). In contrast to adult mammals, lower organisms are capable of regenerating many of their injured organs. For example, zebrafish can regenerate up to 20% of their hearts after surgical amputation primarily through the dedifferentiation and division of pre-existing cardiomyocytes (Jopling et al., 2010; Kikuchi et al., 2010; Poss et al., 2002). Similarly, newts have a remarkable capacity for regenerating a variety of structures, ranging from the heart and ocular lens to a completely functional limb (Laube et al., 2006; Oberpriller and Oberpriller, 1974; Tsonis et al., 2004).

Recent evidence indicates that mice can regenerate their hearts immediately after birth, although this capacity is lost within the first week of life (Porrello et al., 2011b, 2013). These data suggest that the mammalian myocardium retains regenerative potential similar to lower organisms, and understanding the regulatory processes that guide this phenomenon could reveal novel approaches to reactivate this dormant regenerative capacity in adults.

For over a century, it has been reported that nerves play a crucial role in guiding regenerative processes in multiple species. Seminal work in salamander limb regeneration has revealed the reliance on nerves in regeneration (Todd, 1823); if the nerve is severed at the base of the limb prior to or shortly after amputation, the limb will fail to regenerate (Singer, 1952). Studies on the regeneration of a variety of structures in the newt and other organisms have revealed that cholinergic neurons often play a crucial role in the reformation of the severed limb (Drachman, 1964; Singer et al., 1960). More importantly, nerves guide the regeneration of multiple organs in diverse species, suggesting some evolutionarily conserved nerve functions in regeneration (Kumar and Brockes, 2012).

Although cholinergic nerves are critical for multiple regenerative processes, their role in heart regeneration has never been studied. Thus, to determine whether nerve activity is essential for heart regeneration, we used the zebrafish and neonatal mouse models of heart regeneration to address this question. Here, we show that reduction of heart innervation in a transgenic zebrafish model diminishes cardiomyocyte cell-cycle activity and inhibits heart regeneration following injury. Specifically, disruption of cholinergic signaling by pharmacological approaches leads to a reduction in the cardiomyocyte cell-cycle activity of both zebrafish and neonatal mice following injury. We also demonstrate that mechanical ablation of the vagus nerve in the neonatal mouse has a similar effect in inhibiting heart regeneration following apical resection and myocardial infarction. Treatment of mechanically denervated mice with nerve factors rescued the reduced regenerative capacity following

denervation. Finally, transcriptional profiling of the neonatal mouse heart following mechanical denervation revealed patterns for disruption of inflammatory gene expression, which were normally activated during heart regeneration. These factors might contribute to the nerve-dependent regenerative capacity of the heart. These findings reveal that nerve function plays a key role in cardiac regeneration through regulation of cardiomyocyte proliferation.

RESULTS

Innervation Modulates Injury-Induced Cardiomyocyte Proliferation in Zebrafish

The vertebrate heart is innervated during chamber morphogenesis by parasympathetic and sympathetic fibers, which regulate responses of the cardiovascular system to stress. Recent studies indicate that, upon origination from the stellate ganglion, sympathetic nerves are guided along the cardiac surface by neurotrophic signals from developing coronary vascular cells (Nam et al., 2013). We observed extensive innervation of the atrial surface myocardium in adult zebrafish, with less pronounced innervation of the ventricle (Figure 1C, upper panel). After resection of the ventricular apex, new muscle became innervated during regeneration of the new apical wall (Figures 1A and 1B).

To examine the potential involvement of nerves in the regenerative process, we designed transgenic tools to limit the extent of cardiac innervation. We created a transgenic zebrafish line with myocardial overexpression of *semaphorin3aa*, a known inhibitor of cardiac innervation (Ieda et al., 2007) (*Tg(cmlc2:sema3aa)*^{pd106}). As expected, hearts from these animals showed clearly reduced innervation on the ventricular surface (Figure 1C, lower panel), but they appeared otherwise grossly normal. Quantification of surface innervation revealed a 90% reduction in cardiac innervation in *cmlc2:sema3aa* hearts as compared with controls (Figure 1G, n = 5, 6). Following ventricular resection, *cmlc2:sema3aa* hearts displayed a 40% reduction in cardiomyocyte proliferation at 7 days post amputation (dpa), assessed by Mef2/PCNA staining (n = 13, 16; Figures 1D–1F). When assessed at 30 dpa, a time point at which a contiguous wall of heart muscle is typically observed, *cmlc2:sema3aa* animals had a significantly lower regeneration score than wild-type siblings (Figures 1H–1K, n = 9, 11). Thus, hypo-innervated zebrafish hearts display a diminished regenerative response after cardiac injury.

Pharmacological Inhibition of Cholinergic Transmission Reduces Cardiomyocyte Proliferation in Zebrafish and Neonatal Mice

We next designed an experiment to delineate whether cholinergic or adrenergic nerves were responsible for the nerve-dependent heart regeneration phenotypes. We amputated ~20% of the ventricle of zebrafish hearts and then exposed zebrafish to the non-selective muscarinic receptor antagonist atropine (50 μM) to inhibit cholinergic transmission, or the beta-adrenergic receptor antagonist propranolol (50 μM) following apical amputation. We observed many proliferating cardiomyocytes (PCNA/Mef2 double positive) in the regenerate of control zebrafish hearts at 7 dpa (Figure 2A, n = 4). In contrast, resected hearts that were exposed to atropine displayed a marked decrease in the number of proliferating cardiomyocytes (Figure 2B, n = 4). Atropine treatment resulted in a significant reduction in the number of proliferating cardiomyocytes compared to control (Figure 2E, $p < 0.001$). On the other hand, zebrafish treated with the beta-adrenergic antagonist propranolol showed an increase in proliferating cardiomyocytes following amputation similar to controls (Figure 2C, n = 4). To further explore the role of cardiac cholinergic transmission in regeneration, we examined the role of the type 2 muscarinic (M2) receptor, which is the most prevalent type of muscarinic receptor in the heart (Dhein et al., 2001). We treated zebrafish with the M2 receptor-specific antagonist methoctramine. Similar to hearts treated with atropine, we found a decrease in the number of proliferating cardiomyocytes at 7 days post-resection (Figure 2D, n = 4). Quantification showed a significant reduction in the number of proliferating cardiomyocytes in the methoctramine-treated zebrafish (Figure 2E, n = 4). Treatment of zebrafish with atropine, propranolol, and methoctramine alone without injury was used as an additional control. Pharmacological treatment had no impact on zebrafish well-being or on the heart morphology and baseline myocyte proliferation (Figure S1). These data implicate a specific role for cholinergic nerve activity in the proliferation of cardiomyocytes during regeneration.

We have recently reported extensive analysis of the neonatal mouse regenerative response following apical resection (Bryant et al., 2015). Given the demonstration of nerve function in zebrafish myocyte proliferation, we wanted to determine whether inhibition of cholinergic transmission by atropine halts cardiomyocyte proliferation during neonatal mouse heart regeneration. To test this hypothesis, we resected ~15% of the ventricle of 1-day-old neonatal mice and then injected these mice with atropine (5 mg/kg) or vehicle twice daily (Figure 2F). We performed immunostaining against the myocyte marker cardiac troponin t (cTnnt) and the mitosis marker phosphorylated histone H3 (pH3) on histological sections at 7 days post resection (dpr), a time point when cardiomyocyte proliferation is high following injury. Extensive cardiomyocyte proliferation was detected in vehicle-treated mice, while cardiomyocyte proliferation was markedly reduced in atropine-treated mice (Figures 2G and 2H, n = 6–8, $p < 0.005$). To determine the impact on cytokinesis, we performed immunostaining with an antibody against Aurora B kinase, and we detected a significant reduction in the number of cardiomyocytes undergoing cytokinesis in the atropine-treated mice (Figures 2I and 2J, n = 4, $p < 0.05$). There was no significant change in the number of non-myocyte nuclei in both vehicle-and atropine-treated hearts in both sham-operated and resected mice (Figure 2K). Vehicle-treated and atropine-treated sham-operated mice showed comparable body weights; whereas following resection there was a significant reduction in body weight of atropine-treated mice compared to vehicle controls (Figure 2L). Taken together, these results suggest that cholinergic nerve signaling is required for the proliferation of cardiomyocytes during neonatal mammalian cardiac regeneration.

Mechanical Cholinergic Denervation in Neonatal Mice Reduces Cardiomyocyte Proliferation and Impairs Heart Regeneration

Although pharmacological agents represent a powerful tool to interfere with nerve function in the heart, secondary effects may arise due to globally antagonizing cholinergic nerve activity and transmission. In order to exclude non-cardiac effects due to

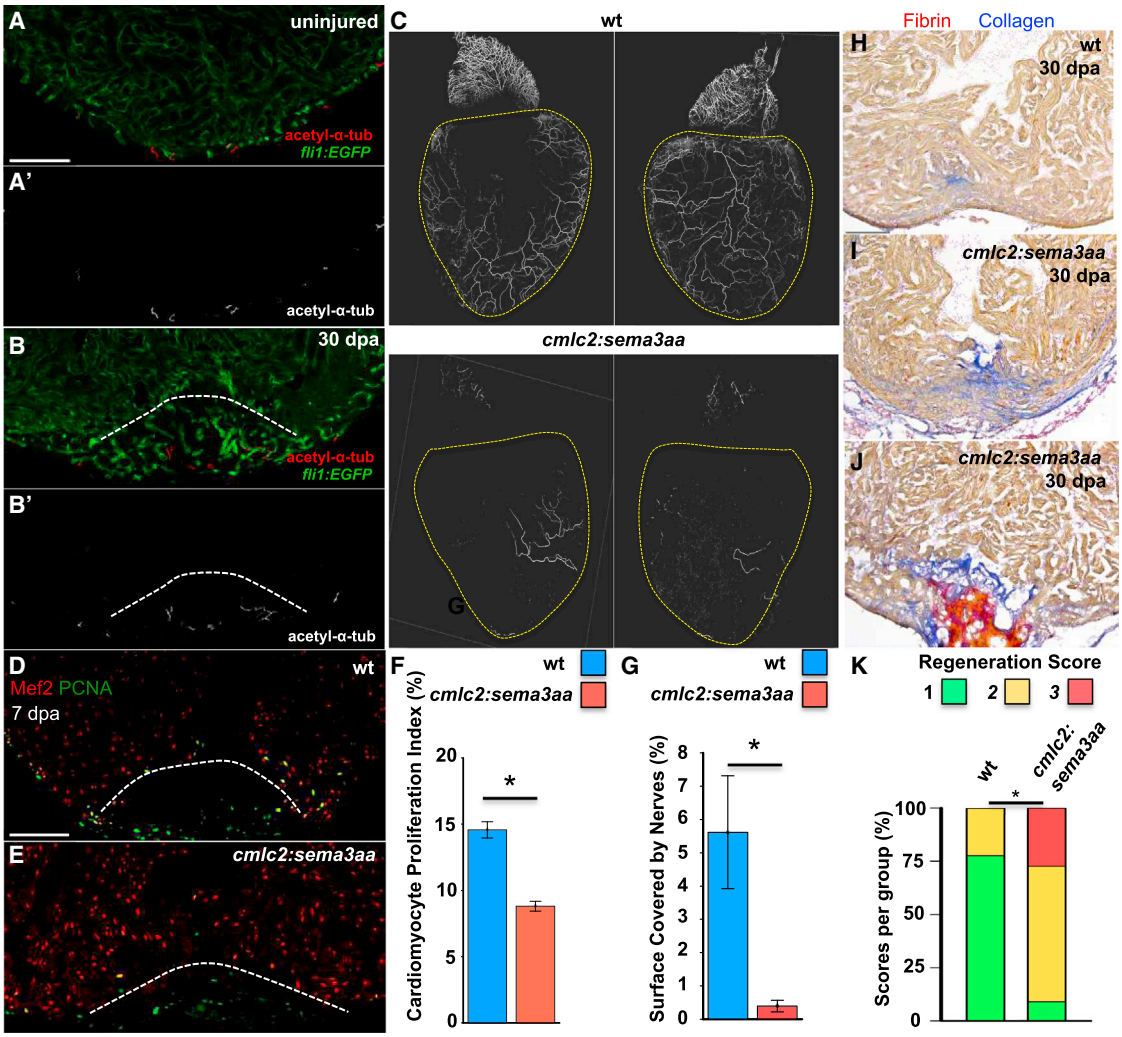

Figure 1. Effects of Cardiac Innervation on Injury-Induced Cardiomyocyte Proliferation

(A and B) Section images of uninjured (A) and regenerated (30 dpa; B) ventricular apices visualized for endothelial cells (green) and nerves (red). The approximate regenerated area is indicated by a dashed line. Grayscale images indicating nerves, positive for acetylated alpha-tubulin, are shown in (A′) and (B′). Scale bar represents 100 μm.

(C) Whole mount images of hearts from wild-type (WT; left) and *cmlc2:sema3aa* (right) animals, immunostained for acetylated alpha-tubulin to indicate cardiac nerves, which are reduced by *sema3aa* overexpression. Scale bar represents 100 μm.

(D and E) Section images of 7 dpa ventricular apices of wild-type (D) or *cmlc2:sema3aa* (E) animals, stained for $Mef2^{+}PCNA^{+}$ cells. Wounds are indicated by dashed lines. Scale bar represents 100 μm.

(F) Quantification of cardiomyocyte proliferation at 7 dpa from hypo-(*cmlc2:sema3aa*). Wild-type clutchmates (n = 16) were used as controls for *cmlc2:sema3aa* animals (n = 13). Data are represented as mean ± SEM. *p < 0.05, Mann-Whitney rank sum.

(G) Quantification of surface innervation as measured by acetylated alpha-tubulin staining, in *cmlc2:sema3aa* (n = 6) and wild-type clutchmate controls (n = 5). Data are represented as mean ± SD. *p < 0.05, Mann-Whitney rank sum.

(H–J) Section images of 30 dpa ventricular apices of wild-type (D) or *cmlc2:sema3aa* (E) animals stained with acid-fuschin orange. Scale bar represents 100 μm.

(K) Quantification of regeneration between *cmlc2:sema3aa* and wild-type siblings were compared at 30 dpa. Hearts (H–J) were scored for regeneration, with 1 indicating complete regeneration (H), 2 indicating partial regeneration (I), and 3 indicating a block in regeneration (J). Data represent percent of total heart per score. *p < 0.05, Fisher's exact.

systemic atropine administration, we developed a surgical procedure in 1-day-old neonatal mice in which we mechanically ablate the left vagus nerve, which directly innervates the heart (Figure 3A). In order to confirm that we specifically dissect out the nerve, the resected nerve portion was immunostained with the pan neuronal marker beta tubulin III (Tubb3); the resected nerve showed positive nerve staining (Figure 3B). Unilateral left vagotomy, but not right vagotomy, has been shown to upregulate M2 receptor expression as a compensatory response in the left atrium and left ventricle following denervation (Chen et al., 2008). To examine whether neonatal left vagotomy caused a similar effect on the expression of M2 receptors, we performed qPCR on the left ventricle at 7 days following vagotomy in neonatal mice. We detected the anticipated upregulation of M2

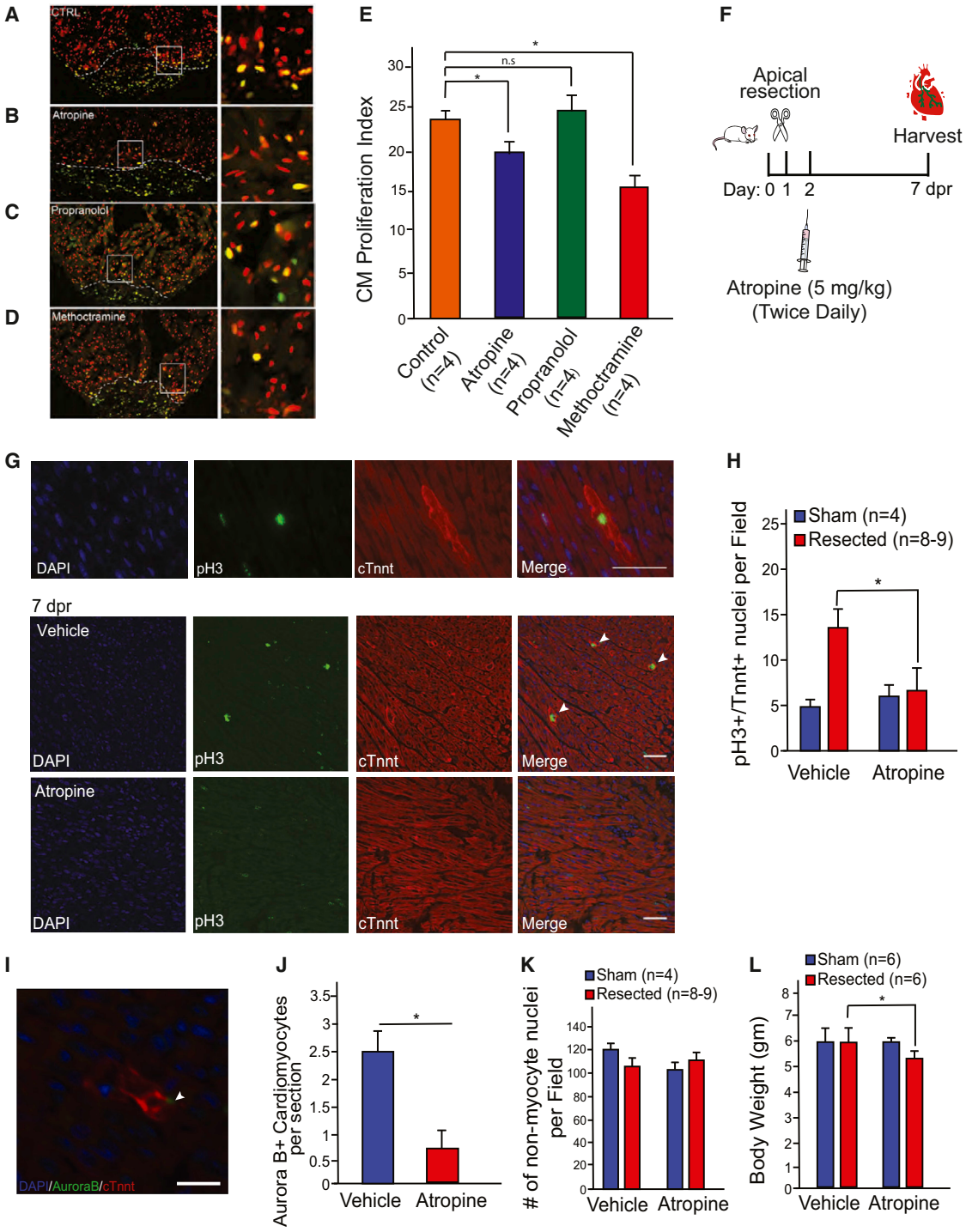

Figure 2. Pharmacological Inhibition of Cholinergic Nerve Function Reduces Cardiomyocyte Proliferation in Zebrafish and Neonatal Mice

(A) Zebrafish hearts were fixed and immunostained for PCNA and Mef2C at 7 days after surgical amputation. Hearts derived from zebrafish treated with water (Control) displayed notable cardiomyocyte proliferation.

(B) Atropine-treated zebrafish exhibited a reduction in proliferating cardiomyocytes.

(C) PCNA and Mef2c staining at 7 dpa for propranolol-treated zebrafish. Control and propranolol-treated zebrafish showed equivalent cardiomyocyte proliferation.

(D) PCNA and Mef2c staining at 7 dpa for methoctramine-treated zebrafish showed significant reduction in cardiomyocyte proliferation. Boxed regions in (A)–(D) are shown at higher zoom in the left panels.

(E) Quantification of proliferating cardiomyocytes showing a significant reduction of the number of proliferating cardiomyocytes in atropine- and methoctramine-treated zebrafish compared to control water- and propranolol-treated zebrafish.

(legend continued on next page)

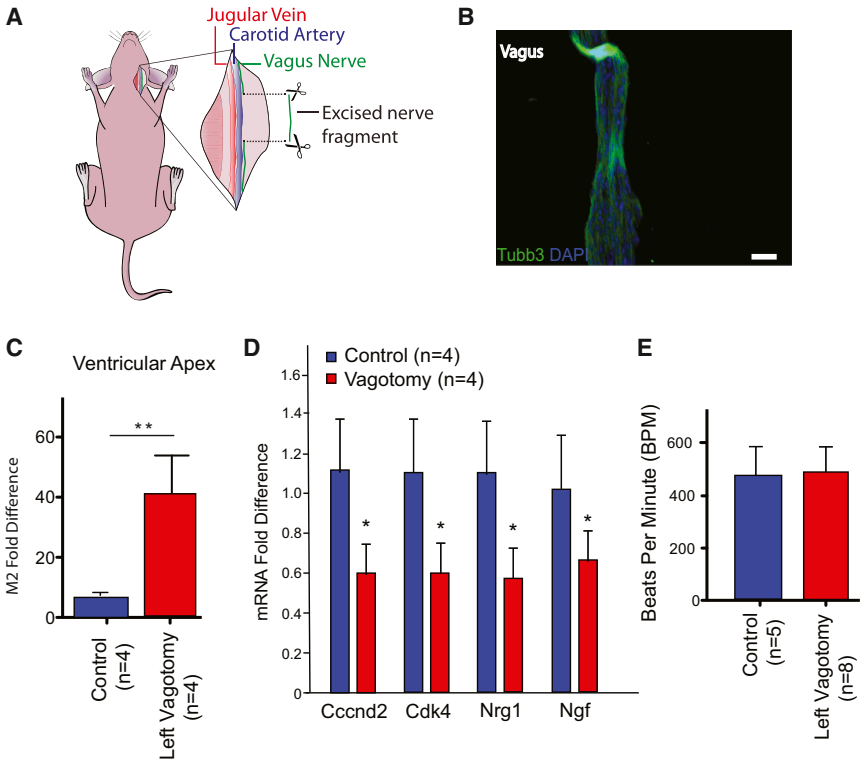

Figure 3. Left Vagotomy as a Model for Mechanical Denervation in the Neonatal Mouse

(A) Schematic depiction of the left vagotomy surgery in neonatal mice.

(B) Immunohistochemistry of the neuronal marker Tubb3 of the resected vagus nerve, nuclei stained with DAPI. Scale bar represents 50 μm.

(C) qPCR gene expression analysis of the M2 receptor levels in sham operated and vagotomized neonatal mice, showing an upregulation of M2 receptor expression following vagotomy.

(D) qPCR expression profile of cell cycle and nerve-secreted factors show significant downregulation in vagotomy compared to unoperated animals ($n = 4$, $p < 0.05$).

(E) Heart rate measurements at 7 days following left vagotomy showing similar heart rates in both control and vagotomized mice.

receptor gene expression in the left ventricular apex of vagotomized neonatal mice (Figure 3C, $n = 4$ per group, $p < 0.01$). These data confirm that left vagotomy in neonatal mice exhibits a similar response to left vagotomy in adult animals and thus represents an approach for mechanical denervation.

To determine whether mechanical cholinergic denervation alone can impact the levels of cardiomyocyte cell-cycle regulators, we performed gene expression analysis of multiple positive regulators of cardiomyocyte cell cycle as *Ccnd2* and *Cdk4* by qPCR (Pasumarthi and Field, 2002). Similarly, we studied growth factors as *Nrg1* and *Ngf* that have been previously shown to enhance cardiomyocyte proliferation (Bersell et al., 2009; Lam et al., 2012). Interestingly, positive regulators of cardiomyocyte cell cycle such as *Ccnd2* and *Cdk4* were significantly downregulated following vagotomy (Figure 3D). In addition, *Nrg1* and *Ngf* were significantly downregulated in the vagotomized neonatal mice (Figure 3D). These data indicate that neonatal mouse vagotomy directly regulates the cardiomyocyte cell-cycle state at the molecular level. To examine whether left vagotomy has an impact on heart rate following vagotomy, we measured the heart rates of mice at 7 days post vagotomy. We found no significant differences in the heart rates of control and vagotomized mice at resting conditions (Figure 3E).

We performed a double surgical procedure where neonates undergo vagotomy paired with apical resection to assess whether vagotomy compromises neonatal heart regeneration. Interestingly, the neonatal mice that underwent apical resection paired with vagotomy of the heart showed lower levels of proliferating cardiomyocytes, similar to both sham operated and vagotomized mice (Figure S2A). Quantification of the pH3 positive cardiomyocytes showed a significant decrease in the number of proliferating cardiomyocytes in resected plus vagotomized mice compared to resection alone (Figure S2B, $n = 5$, $p < 0.05$).

Similar to regeneration following apical resection, neonatal mice have the capacity to regenerate their hearts following myocardial infarction (MI), a major cause of heart failure in humans (Mahmoud et al., 2014; Porrello et al., 2013). We performed both MI + vagotomy on 1-day-old mice (Figure 4A). Interestingly, the mice that underwent the double surgery had a higher mortality rate compared to either vagotomy or MI alone. Kaplan-Meier survival analysis showed that combined vagotomy and MI significantly increased mortality (Figure 4B). At day 7 following MI + vagotomy, immunohistochemistry of pH3 and cTnnt showed reduction of proliferating cardiomyocytes in the MI + vagotomy mice compared to MI alone (Figures 4C and 4D, $n = 4$–6,

(F) Schematic of atropine injection strategy in neonatal mice.

(G) Mouse hearts were fixed and immunostained for phospho-histone H3 (pH3) and cardiac troponin T (cTnnt) at 7 dpr in vehicle- and atropine-treated mice. The upper panel shows a high-magnification image of a pH3+ cardiomyocyte. Scale bar represents 50 μm.

(H) Quantification of the number of proliferating cardiomyocytes at 7 days post apical resection showing a significant decrease of proliferating cardiomyocytes in neonatal mice.

(I) Immunostaining of Aurora B and cTnnt. Scale bar represents 50 μm.

(J) Quantification of the Aurora B+ cardiomyocytes showing a significant reduction in the number of Aurora B+ cardiomyocytes in atropine-treated mice.

(K) Quantification of the number of nuclei in heart sections of vehicle- and atropine-treated mice showing no significant differences between treatments.

(L) Body weights of vehicle- and atropine-treated mice following sham and resection showing a significant reduction in body weights of atropine-resected mice but no changes in sham-operated mice. Data presented as mean ± SEM, where $p < 0.05$ was considered statistically significant.

See also Figure S1.

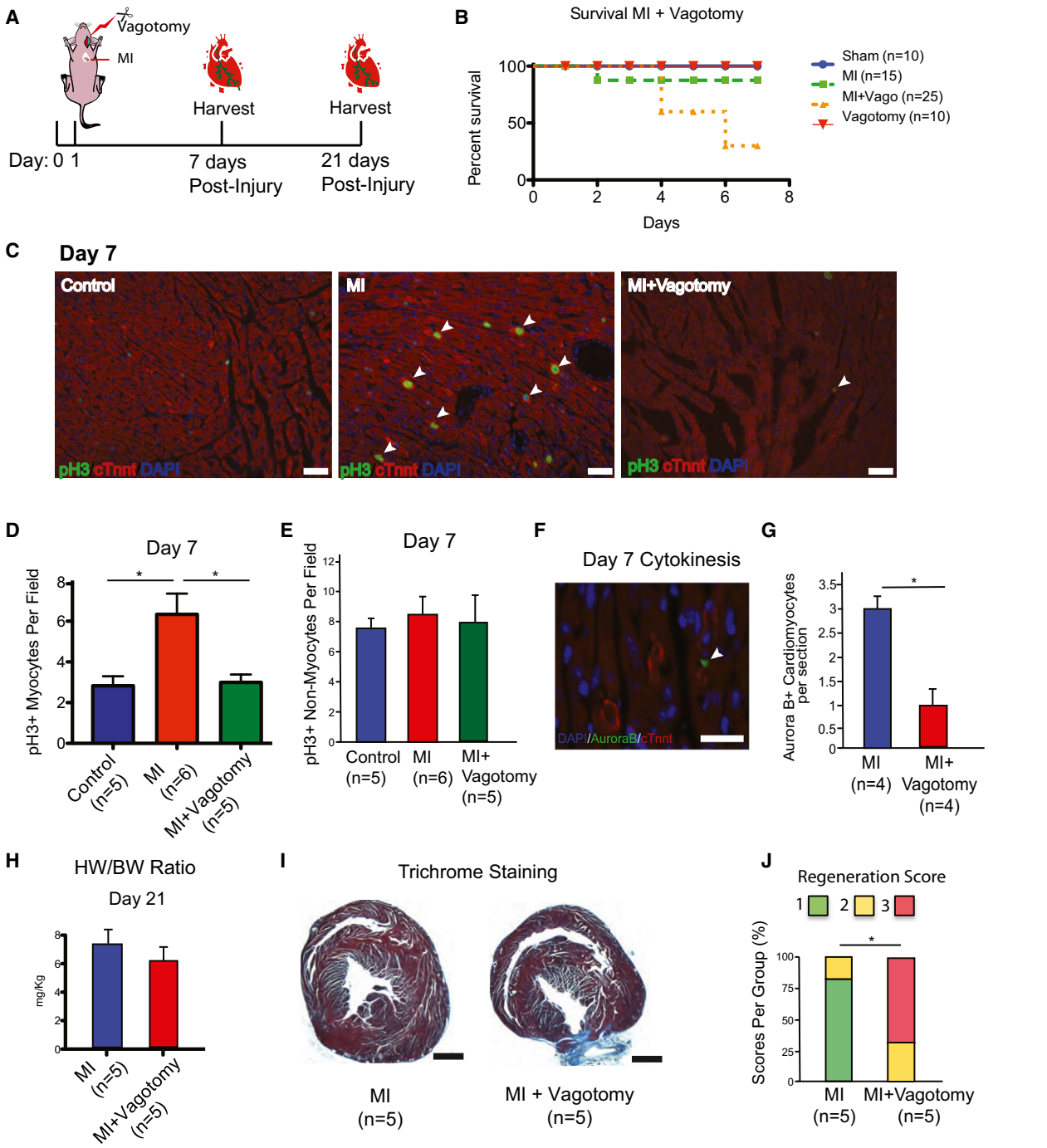

Figure 4. Mechanical Denervation Reduces Cardiomyocyte Proliferation and Heart Regeneration in the Neonatal Mouse

(A) Schematic of neonatal vagotomy and myocardial infarction strategy in neonatal mice.

(B) Kaplan-Meier survival curve of MI and MI + vagotomy mice. A significant reduction in survival of MI + vagotomy mice was observed as assessed by Kaplan-Meier analysis.

(C) Immunostaining of pH3 and cTnnt showing high levels of proliferating myocytes in MI hearts at 7 dpr, while a marked decrease in the levels of proliferating cardiomyocytes in MI + vagotomy hearts. Scale bar represents 50 μm.

(D) Quantification of the number of proliferating cardiomyocytes showing a significant decrease of proliferating cardiomyocytes following vagotomy and myocardial infarction.

(E) Quantification of the number of proliferating non-myocytes showing no significant changes between groups.

(F) Immunostaining of Aurora B and cTnnt.

(G) Quantification of the number of Aurora B cardiomyocytes showing a significant reduction in the number of Aurora B+ cardiomyocytes following MI + vagotomy.

(legend continued on next page)

$p < 0.05$). No significant changes were observed in the number of proliferating non-myocytes (Figure 4E). In addition, there was a significant reduction in the number of cardiomyocytes undergoing cytokinesis as detected by Aurora B staining (Figures 4F and 4G, $n = 4$, $p < 0.05$). There was a trend toward a decrease in the heart weight to body weight (HW/BW) ratio of MI + vagotomy mice compared to MI only, but this trend was not statistically significant (Figure 4H).

To further establish the effects of mechanical denervation on neonatal heart regeneration, we performed Trichrome staining 21 days post injury to assess regeneration and fibrosis in both MI + vagotomy mice compared to either MI or sham-operated mice. The MI + vagotomy mice demonstrated little to no regrowth below the ligated plane of the heart with the presence of a fibrotic scar (Figure 4I). In contrast, animals that had undergone MI alone demonstrated complete heart regeneration with little to no scar formation (Figure 4I). Quantification of regeneration showed a significantly reduced regeneration score following MI + vagotomy (Figure 4J, $n = 5$). To determine whether levels of cardiac innervation are changed beyond the regenerative window, we performed immunostaining of cardiac nerves with the neuronal marker Neurofilament in both P1 and P21 hearts and detected similar patterns of innervation (Figure S3). Collectively, our results show that mechanical ablation of nerves can inhibit the neonatal mouse cardiac regenerative response, which highlights the intimate involvement of nerves during heart regeneration.

Rescue of Mechanically Denervated Hearts by Neuregulin1 and Nerve Growth Factor

To test whether acetylcholine (Ach) as well as the growth factors neuregulin1 (NRG1) and nerve growth factor (NGF) can stimulate cardiomyocyte proliferation, we treated cultured neonatal rat ventricular cardiomyocytes with these factors for 48 hr and measured DNA synthesis by ^{3}H-thymidine incorporation (Figure 5A). NRG1 was able to increase cardiomyocyte DNA synthesis, but not acetylcholine or NGF (Figure 5B). These data suggest that acetylcholine cannot directly stimulate cardiomyocyte proliferation at the M2 muscarinic receptor level, while NRG1 can directly induce myocyte DNA synthesis as has been previously established (Bersell et al., 2009). Although NGF did not cause a significant induction of myocyte DNA synthesis, it has been shown to enhance recovery post injury suggesting that NGF may enhance cardiac repair indirectly (Lam et al., 2012; Meloni et al., 2010). This suggests that NGF may enhance cardiac repair indirectly.

To determine whether inhibition of regeneration by mechanical denervation could be partly rescued through NRG1 and NGF, we injected these recombinant proteins in neonatal mice post MI + Vagotomy (Figure 5C). At 7 days post injury, there was a significant increase in the number of pH3 positive cardiomyocytes in the treated mice compared to controls (Figures 5D and 5E, $n = 4–5$, $p < 0.05$). A significant increase in the number of cardiomyocytes undergoing cytokinesis as determined by Aurora B staining was detected as well (Figures 5F and 5G, $n = 4$, $p < 0.05$). At 21 days post injury, there was reduced scar formation in the NRG1- and NGF-treated mice (Figure 5H, $n = 6$). Quantification of regeneration showed a significantly higher regeneration score in the NRG1- and NGF-treated mice (Figure 5I). These data suggest that nerves stimulate heart regeneration partly through growth factors as indicated by supplying recombinant NRG1 and NGF following mechanical denervation.

To examine whether cholinergic stimulation can enhance regeneration in vivo, we performed MI at P7, a time point when myocyte proliferation and regeneration is limited (Porrello et al., 2013). We injected the mice with the cholinergic agonist carbachol for 7 days (Figure 5J). At 7 days post injury, no significant difference in cardiomyocyte proliferation was detected (Figures 5K and 5L, $n = 5–6$). These data suggest that cholinergic stimulation in vivo does not appear sufficient to induce cardiomyocyte proliferation.

Mechanical Denervation Disrupts Inflammatory Gene Expression following Apical Resection in the Mouse

To gain insight into the early factors that might be responsible for nerve-dependent heart regeneration, we performed expression analysis on the heart ventricular apex from animals that had undergone sham operation, apical resection, or apical resection and left vagotomy. RNA was extracted from the ventricular apex 24 hr after surgery, and RNA sequencing (RNA-seq) was performed. As previously reported, apical resection stimulates a strong immune response 24 hr post surgery (Aurora et al., 2014; O'Meara et al., 2015). The most striking difference in gene expression between resected and resected plus vagotomy was the blunted expression of inflammatory genes activated upon resection (Figure 6A). Genes that were significantly upregulated in resected versus sham hearts and also significantly downregulated in resected + vagotomy versus resected hearts fell into gene ontology biological processes such as immune response, response to wounding, and chemotaxis (Figure 6B). Specifically, genes involved in the innate immune response and chemotaxis (IL1b, Cxcl5, and Pf4) were downregulated to almost baseline levels (Figure 6C). On the other hand, expression of several immune genes involved in lymphocyte-mediated immunity and adaptive immune response (Icam-1, Slc11a1, Bcl6, and Nfkb2) was not blunted in response to vagotomy. A large subset of genes showed similar expression patterns in sham and resected hearts but were upregulated (translation, RNA processing) or downregulated (proteolysis, catabolic processes) after vagotomy. These genes are not likely related to the nerve-dependent regeneration phenotype since they were not modulated upon resection alone. To determine whether similar

(H) Heart weight to body weight (HW/BW) ratio showing slightly reduced but not significant difference in the MI + vagotomy heart.

(I) Trichrome staining of MI + vagotomy and MI hearts at 21 dpr, showing incomplete regeneration and persistence of a fibrotic scar in vagotomized mice. Scale bar represents 1 mm.

(J) Quantification of regeneration in MI and MI + vagotomy mice. 1 indicates complete regeneration, 2 indicates partial regeneration, and 3 indicates a block in regeneration. Data represent total heart per score, 2×3 contingency analysis, $p < 0.05$. Data presented as mean ± SEM, where $p < 0.05$ was considered statistically significant.

See also Figures S2 and S3.

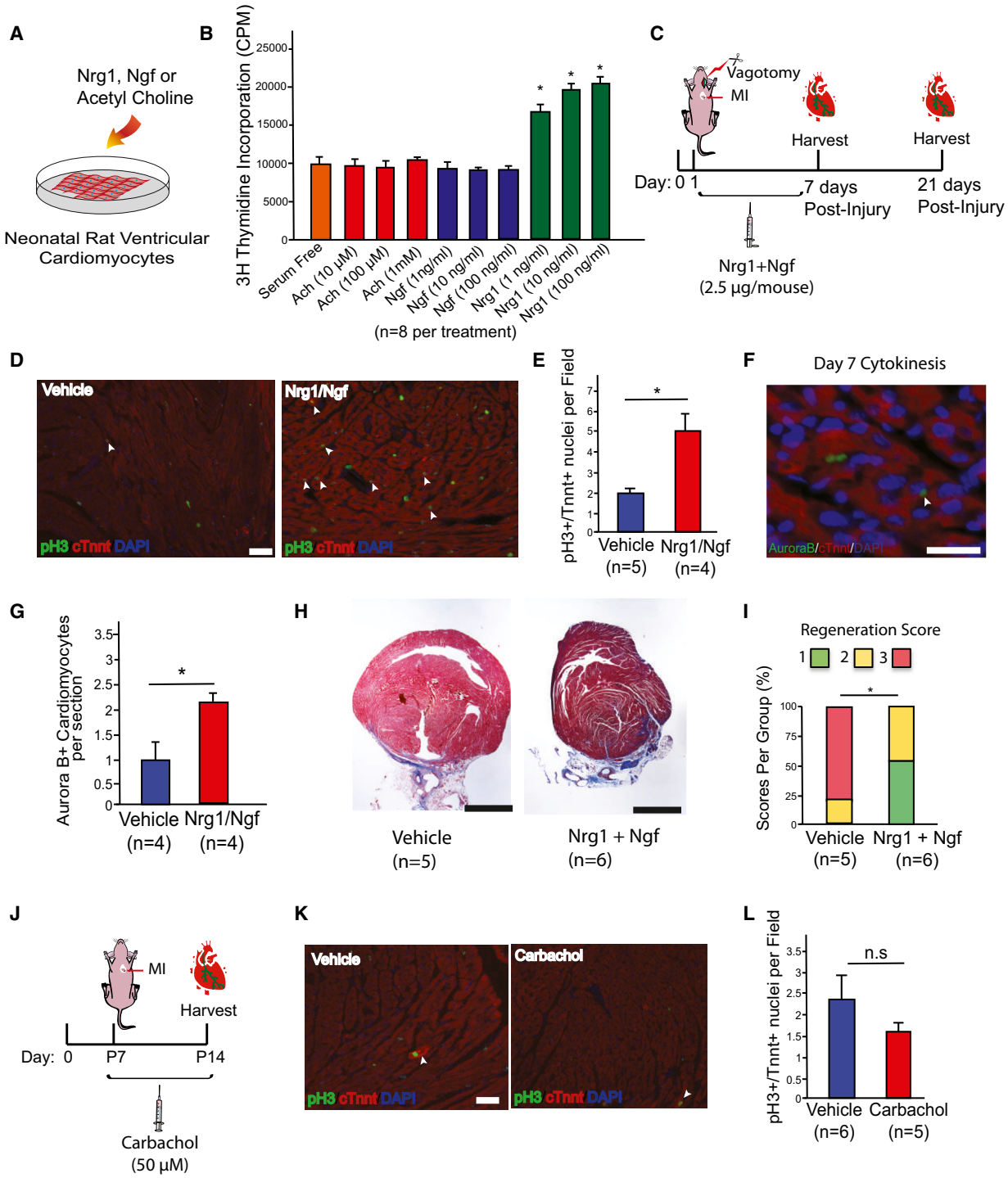

Figure 5. Rescue of Mechanically Denervated Mice by NRG1 and NGF

(A) Schematic of neonatal rat cardiomyocyte treatment with acetylcholine (Ach), NRG1, and NGF.

(B) ^{3}H thymidine incorporation showing increased DNA synthesis in cardiomyocytes treated with NRG1, but not acetylcholine or NGF.

(C) Schematic of injections of recombinant NRG1 and NGF in neonatal mice following MI + vagotomy.

(D) Immunostaining of pH3 and cTnnt showing high levels of proliferating myocytes in treated mice at 7 days post injury compared to controls. Scale bar represents 50 μm.

(E) Quantification of the number of proliferating myocytes following NRG1 and NGF injection showing higher number of proliferating myocytes compared to controls.

(F) Immunostaining of Aurora B and cTnnt. Scale bar represents 50 μm.

(legend continued on next page)

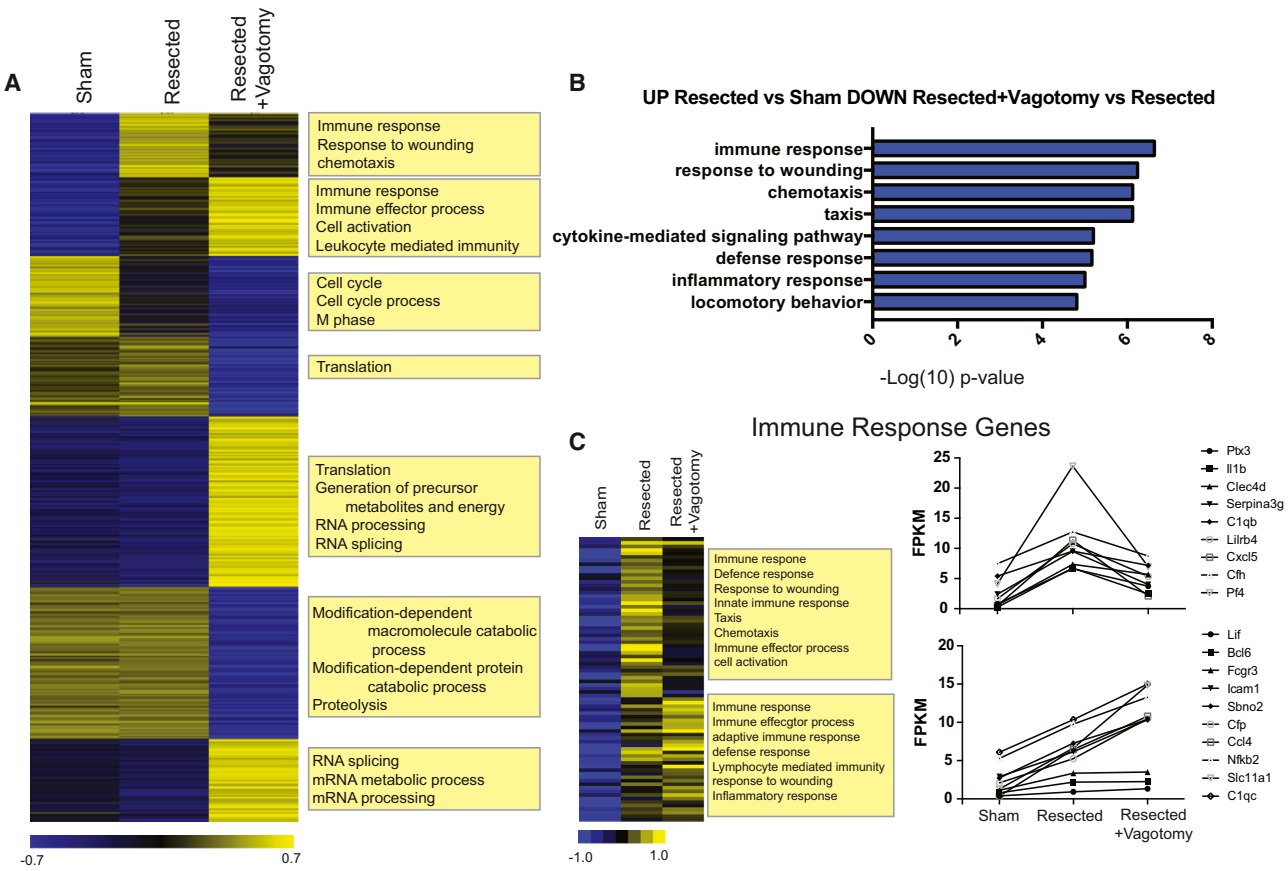

Figure 6. Immune Response Genes Are Differentially Expressed following Mechanical Denervation

(A) K-means clustering of all genes differentially expressed across hearts from animals that had undergone sham operation, apical resection, or apical resection and left vagotomy surgeries.

(B) Gene ontology biological processes of genes significantly upregulated in resected versus sham hearts and also significantly downregulated in resected + vagotomy versus resected hearts.

(C) K-means clustering and FPKM plots of Immune response genes significantly upregulated in resected versus sham hearts.

See also Figure S4.

transcriptional changes that regulate cholinergic-mediated cardiac regeneration are conserved across species, we performed a microarray on atropine-treated zebrafish at 24 hr following resection. Interestingly, there was a significant downregulation of immune response genes in the atropine-treated zebrafish compared to control (Figure S4). These data suggest that immune function plays an important role in both zebrafish and heart regeneration, and in both models the immune response is blunted by cholinergic inhibition. Collectively, our results reveal a requirement for nerves in guiding cardiac regeneration in both zebrafish as well as neonatal mice by regulating cardiomyocyte proliferation (Figure 7).

DISCUSSION

Multiple species throughout the animal kingdom mediate their regenerative response through nerve activity; we sought to explore whether similar mechanisms are evolutionarily conserved in heart regeneration (Kumar and Brockes, 2012). Our data demonstrate that nerves are required for cardiomyocyte

(G) Quantification of the number of Aurora B cardiomyocytes showing a significant increase in the number of Aurora B+ cardiomyocytes in NRG1-/NGF-treated mice compared to controls.

(H) Trichrome staining at 21 days post injury, showing reduced scare in NRG1- and NGF-treated mice. Scale bar represents 1 mm.

(I) Quantification of regeneration in vehicle-and NRG1 + NGF-treated mice showing a significant higher regeneration scores in NRG1 + NGF-treated mice. 1 indicates complete regeneration, 2 indicates partial regeneration, and 3 indicates a block in regeneration. Data represent total heart per score, 2 × 3 contingency analysis, $p < 0.05$.

(J) Schematic of carbachol injections following MI at P7.

(K) Immunostaining of pH3 and cTnnt to detect mitotic cardiomyocytes. Scale bar represents 50 μm.

(L) Quantification of mitotic cardiomyocytes showing no significant increase in myocyte cell-cycle activity in carbachol-treated mice. Data presented as mean ± SEM, where $p < 0.05$ was considered statistically significant.

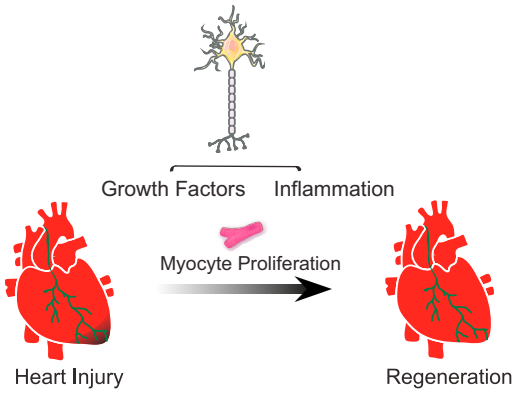

Figure 7. Proposed Model of Nerve Dependence of Heart Regeneration

A schematic showing the proposed role that nerves play on cardiomyocyte proliferation and the impact of pharmacological, genetic, and mechanical denervation on heart regeneration.

proliferation and heart regeneration of both zebrafish and neonatal mice. Hypo-innervation of the adult zebrafish heart using transgenic zebrafish reduces myocyte proliferation and heart regeneration. Pharmacological inhibition of cholinergic nerve function reduces cardiomyocyte cell-cycle activity in both zebrafish and neonatal mice. In addition, we demonstrate that mechanical denervation of the left vagus nerve in neonatal mice reduces cell-cycle gene expression, cardiomyocyte proliferation, and prevents heart regeneration following both apical resection and myocardial infarction suggesting a critical role for cholinergic nerve activity in heart regeneration. Administration of recombinant proteins of NRG1 and NGF increases cardiomyocyte proliferation and enhances regeneration following denervation. RNA-seq analysis of mechanically denervated hearts demonstrates a significant impact of denervation on inflammatory pathways gene expression. A similar effect was observed in zebrafish following pharmacological inhibition of cholinergic nerve function.

This study sheds light on a requirement for nerves in regulating cardiomyocyte proliferation and heart regeneration in lower vertebrates and mammals. Nerves appear to be essential for the homeostasis of the adult human heart as well, due to re-innervation of the adult human heart post transplantation (Cornelissen et al., 2012; Gallego-Page et al., 2004). Recent studies have uncovered multiple regulators of mammalian cardiac regeneration (Aurora et al., 2014; Chen et al., 2013; Eulalio et al., 2012; Heallen et al., 2013; Mahmoud et al., 2013; Porrello et al., 2011a; Puente et al., 2014; Xin et al., 2013), yet the differences and/or similarities of evolutionary conserved regenerative mechanisms between lower organisms and mammals is not yet clear. We demonstrate that the impact of nerves seems to affect both the expression of growth factors as well as the inflammatory response post injury. Owing to the established role of semaphorin signaling in vascular patterning (Epstein et al., 2015), it is not clear whether a vascular mechanism is involved in the regenerative response as well. Interestingly, modulating expression of growth factors as Ngf by cholinergic signaling has been reported following cholinergic denervation in the brain (da Penha Berzaghi et al., 1993; Lapchak et al., 1993), suggesting interplay between cholinergic nerves and Nrg1 and Ngf activity. Recent reports identified Nrg1 as an inducer of myocyte proliferation in zebrafish, as well as in mice within the first week of birth, through the Nrg1 co-receptor Erbb2 (D'Uva et al., 2015; Gemberling et al., 2015; Polizzotti et al., 2015). Our rescue experiments with NRG1 and NGF indicate that administration these factors may partially rescue the effect of denervation, but whether these factors specifically mediate the nerve effect is unclear. Attempts at identifying nerve-derived factors during regeneration have been pursued, but their exact role in different species is not completely understood (Kumar and Brockes, 2012; Kumar et al., 2007). It remains to be determined whether nerves directly release these mitogens, or regulate their expression. In addition, the impact of cholinergic signaling on inflammation has been previously studied (Martelli et al., 2014). The role of the immune system has been shown to mediate a proper regenerative response following injury as well (Aurora et al., 2014; Godwin et al., 2013; Lavine et al., 2014) perhaps suggesting interplay between cholinergic nerves and immune response in facilitating heart regeneration. Collectively, our study identifies a dual role of nerves in heart regeneration in both lower vertebrates and mammals by regulating mitogen and inflammatory gene expression following injury.

EXPERIMENTAL PROCEDURES

Experimental Animals

All experiments were conducted in accordance with the Guide for the Use and Care of Laboratory Animals and approved by the Harvard Medical School Standing Committee on Animals. Timed-Pregnant ICR/CD1 mice used to deliver pups were obtained from Charles River Laboratories.

Zebrafish Amputations

Adult zebrafish from 3–5 months were used for apical amputations as described previously (Poss et al., 2002).

Neonatal Mouse Apical Resection and Myocardial Infarction

Neonatal mouse apical resections and myocardial infarctions were performed on 1-day-old and 7-day-old pups as described previously (Mahmoud et al., 2014).

Neonatal Mouse Vagotomy

Neonatal mice were anesthetized on ice. The neck area was cleaned three times alternately using alcohol and betadine in preparation for surgery. A lateral incision of about 5 mm was made ~2–3 mm from the clavicle on the left center side of the throat. The lobes of the salivary glands were gently separated and the fascia and fatty tissue were separated until the carotid jugular bundle was visualized. The carotid artery and jugular vein were gently isolated until the vagus nerve was visible. The vagus nerve was firmly grasped and pulled toward the head of the mouse until the vagus broke. A segment of ~3–6 mm is sufficient to ensure complete separation with little chance of reattachment. Mice that had resection of a smaller part of the vagus were excluded from the analysis.

Administration of Pharmacological Agents

For zebrafish experiments, atropine was mixed with tank water and changed daily. Atropine or propranolol was added at a concentration of 50 μM. Methoctramine was added at a concentration of 50 nM.

For neonatal mice, atropine was dissolved in PBS and administered to neonatal mice following apical resection at P1 by intraperitoneal injections twice daily at a concentration of 5 mg/kg. Carbachol was injected at a concentration of 50 μM. PBS administration was used as vehicle.

Generation of Transgenic Lines

cmlc2:sema3aa

sema3aa cDNA was amplified with the primers 5′-ACAATGGATTACC TTGTTGG-3′ and 5′-ACATTACACGCTGCGTGGTGG-3′ and subcloned

behind the 5.1 kb *cmlc2* (*myl7*, Zebrafish Information Network) promoter (Rottbauer et al., 2002). The cassette was co-injected into one-cell stage wild-type embryos with I-SceI. Two founders were isolated and propagated. The full name of this transgenic line is *Tg(cmlc2:sema3aa)*^{pd106}.

Histological Analysis

Primary and secondary antibody staining was performed as described (Kikuchi et al., 2011). Whole mount nerve staining was performed as follows. Heart were fixed in 4% PFA for 1 hr at room temperature with atria removed. Heart were then washed 4 × 5 min with PBS that contained 0.3% tween-20 (PBT). Hearts were placed in blocking media (0.3% PBT, 2% horse serum, 1% DMSO, and 10% calf-serum [heat inactivated]) for 2 hr at room temperature at 4°C on rotator. Block media was removed and replaced with antibody staining solution (0.3% PBT, 1% DMSO, 1:100 acetylated alpha-tubulin, and 10% calf-serum [heat inactivated]) overnight at 4°C. Hearts were then placed in mounting media between coverslips for imaging.

Acid fuchsin-orange G staining was performed on 10-μm sections as described (Poss et al., 2002). Mef2/PCNA staining on sections from 7 dpa ventricles was performed and imaged as described (Kikuchi et al., 2011). Mef2$^+$ and Mef2$^+$/PCNA$^+$ cells were counted manually. The three largest injuries from each heart were averaged to compute a proliferative index for each animal. Primary antibodies used in this study: anti-PCNA (mouse; Sigma) at 1:250, anti-Mef2 (rabbit; Santa Cruz Biotechnology) at 1:75, and anti-acetylated alpha-tubulin (mouse; Sigma) at 1:100. Secondary antibodies used in this study: Alexa Fluor 594 goat anti-mouse IgG (H$^+$L) for anti-Mef2, anti-PCNA, and anti-acetylated alpha-tubulin; and Alexa Fluor 488 goat anti-rabbit IgG (H$^+$L) for anti-Mef2 and anti-PCNA. Secondary antibodies (Invitrogen) were all used at 1:200.

Mouse hearts were fixed in 4% paraformaldehyde and paraffin embedded. Paraffin sections were deparaffinized in xylene and rehydrated by graded alcohols, followed by antigen retrieval with antigen retrieval citrate solution (DAKO) in boiling water for 20 min. Slides were cooled at room temperature for 30 min; sections were blocked with 10% goat serum, and incubated with pH3 (Millipore, 1:200), Aurora B (Sigma, 1:100) cardiac Tnnt (Abcam, 1:200), and Tubb3 (Abcam, 1:500) antibodies overnight at 4°C. The following day, sections were washed with PBS and incubated with corresponding secondary antibodies conjugated to Alexa Fluor 488 and Alexa Fluor 568 (Invitrogen).

Trichrome staining was performed on neonatal mouse hearts fixed in 4% paraformaldehyde and paraffin embedded. Sections were deparaffinized, placed in Bouin's fluid at 60°C for 1 hr, and then rinsed for 5 min in deionized water. Sections were then stained with iron hematoxylin for 10 min then rinsed in deionized water for 10 min. Sections were stained with Biebrich scarlet-acid fuchsin solution for 5–10 min then rinsed in deionized water for 30 s. Sections were placed in phosphotungstic-phosphomolybdic acid solution for 5 min, and then stained in Aniline Blue for 5–10 min. Slides were placed in 1% acetic acid for 1 min, rinsed in deionized water for 30 s, followed by dehydration in alcohol for 2 min, then mounted with a coverslip.

Quantification of Innervation

Whole mount images obtained from *cmlc2:sema3aa* hearts and controls stained with acetylated-alpha tubulin, were imported into Photoshop and merged using the photomerge function. Subsequent brightness and contrast adjustments were made to allow for proper masking of the nerves. Images were then imported to ImageJ, where thresholding was set to define the area of the nerves. Masks for total area of the heart and nerve area were quantified using ImageJ. Nerves were quantified by calculating the total area of the nerves divided by the total area of the surface of the heart to calculate a percent nerve area. Quantification was performed for the surface of the heart opposite the valve.

Quantification of Regeneration

Regenerates were scored on a scale from 1 to 3 after acid-fuschin orange staining for zebrafish and trichrome staining for mice. "1" indicated complete regeneration (signified by contiguous muscle and little to no scarring), "2" indicated partial regeneration (signified by moderate scarring and partial muscle regeneration), and "3" indicated a block in regeneration (clear gap in ventricular wall, filled by fibrin and scar). Representative images from each animal were scored by three individuals blinded to the identities of the animals. The average score for each heart was calculated and rounded to the nearest whole number.

Real-Time PCR

Total RNA was isolated from zebrafish and mouse hearts using Trizol (Invitrogen) and reverse transcription for cDNA synthesis was performed using random hexamer primers with the High-Capacity cDNA Reverse Transcription Kit (Invitrogen). Validated primers from MGH primer bank (http://pga.mgh.harvard.edu/primerbank/) were ordered from Integrated DNA Technologies. Real-time PCR was performed with SYBR Green (Applied Biosystems) on CFX384 Touch Real-Time PCR detection system (Bio-Rad). GAPDH, beta-actin, and 18S were used as a loading control to normalize gene expression using the ΔΔCt method.

RNA-Seq and Analysis

At 24 hr post procedure, neonatal mouse hearts were isolated and perfused in 1× PBS. Total RNA was extracted from the lower half of the ventricle using Trizol (Invitrogen) according to the manufacturer's protocol. The Poly(A) mRNA Isolation Module (Wafergen, #400047) was used to isolate poly-adenylated RNA from 0.2 to 1.0 μg of total RNA. The polyadenylated RNA was fragmented, and the first and second strand synthesis were performed on a Wafergen Apollo 324 System using the IntegenX Directional PrepX mRNA kit (IntegenX). The addition of barcodes and minimal library amplification were done using PCR. Library clustering and paired-end (50-bp read lengths) sequencing were performed on an Illumina HiSeq 2500. Three biological replicates for each group (sham, resection, and resection + vagotomy) were processed and sequenced as described above. Sequencing reads were aligned to the GRCm38 mouse genome using Tophat (Kim et al., 2013). Cufflinks was used to assemble transcripts and to estimate transcript abundances, which are measured in fragments per kilobase per million fragments mapped (FPKM) (Trapnell et al., 2010). A q value cutoff of 0.05 was used to determine the statistical significance of differentially expressed genes. The heatmaps were generated in Java Treeview (Saldanha, 2004). Gene ontology (GO) categories were determined using the Database for Annotation, Visualization, and Integrated Discovery (DAVID) (Huang et al., 2009a, 2009b). Benjamini-Hochberg-corrected p values are reported for enriched biological processes. RNA-seq data have been uploaded to the Gene Expression Omnibus (GEO: GSE69855).

Isolation, Culture, and Treatment of Neonatal Rat Cardiomyocytes

Rat ventricular cardiomyocytes were isolated from P1 neonatal Sprague-Dawley rats as previously described (Liao and Jain, 2007). Cardiomyocytes in serum-free media were treated with multiple doses of acetylcholine, NRG1 (R&D), and NGF (Sigma) followed by quantificataccesion of ^{3}H thymidine incorporation.

^{3}H Thymidine Incorporation

To quantify ^{3}H thymidine incorporation, we treated cardiomyocytes with ^{3}H thymidine 24 hr before collection. Cells were washed with PBS and lysed with 0.1 M NaOH + 0.1% SDS. Quantification was performed using the LS 6500 Scintillation Counter (Beckman Coulter).

Statistical Analysis

All data are presented as mean ± SEM. Student's unpaired t test or one-way ANOVA was used for comparisons between two groups unless otherwise noted. A value of $p < 0.05$ was considered significant.

ACCESSION NUMBERS

The accession numbers for the RNA-seq data reported in this paper are GEO: GSE69855, GSE69775.

SUPPLEMENTAL INFORMATION

Supplemental Information includes Supplemental Experimental Procedures and four figures and can be found with this article online at http://dx.doi.org/10.1016/j.devcel.2015.06.017.

AUTHOR CONTRIBUTIONS

A.I.M. and C.C.O. designed and performed the experiments, analyzed the data, made the figures, and wrote the paper. M.G., W.C., G.F.E., and K.D.P. generated the cmlc2:sema3aa zebrafish and assessed cardiac innervation and heart regeneration in these animals. L.Z., R.Z., D.M.B., J.B.G., and L.C. performed experiments. C.E.B., C.G.B., and C.A.M. supervised experiments and edited the paper. R.T.L. conceived the study, designed experiments, and wrote and edited the paper.

ACKNOWLEDGMENTS

We thank the R.T.L. and K.D.P. laboratory members for helpful discussions, J. Burris, N. Blake, S. Davies, and A. Dunlap for zebrafish care, and A. Dickson for quantitative analysis of images. This work was supported by an American Heart Association Postdoctoral fellowship (15POST21870000 to A.I.M.), NIH F32HL117595 Postdoctoral Fellowship (C.C.O.), and an HHMI Gilliam Fellowship (D.M.B.). M.G. was supported by a fellowship from the American Heart Association (AHA). L.Z. was supported by a fellowship from the AHA (14POST20380738). W.Y.C. was supported by a fellowship from the NIH (F32 HL106987-02). This work was supported by grants from the NIH (HL127067 to C.E.B. and C.G.B., HL081674 to K.D.P., and AG040019 and HL117986 to R.T.L.).

Received: June 12, 2014
Revised: May 7, 2015
Accepted: June 18, 2015
Published: August 6, 2015

REFERENCES

Aurora, A.B., Porrello, E.R., Tan, W., Mahmoud, A.I., Hill, J.A., Bassel-Duby, R., Sadek, H.A., and Olson, E.N. (2014). Macrophages are required for neonatal heart regeneration. J. Clin. Invest. *124*, 1382–1392.

Bersell, K., Arab, S., Haring, B., and Kühn, B. (2009). Neuregulin1/ErbB4 signaling induces cardiomyocyte proliferation and repair of heart injury. Cell *138*, 257–270.

Bryant, D.M., O'Meara, C.C., Ho, N.N., Gannon, J., Cai, L., and Lee, R.T. (2015). A systematic analysis of neonatal mouse heart regeneration after apical resection. J. Mol. Cell. Cardiol. *79*, 315–318.

Chen, L.N., Zang, W.J., Yu, X.J., Liu, J., Li, D.L., Kong, S.S., Lu, J., and Xu, X.L. (2008). Compensatory recovery of vagal control of hemodynamics after unilateral vagotomy. Physiol. Res. *57*, 119–132.

Chen, J., Huang, Z.P., Seok, H.Y., Ding, J., Kataoka, M., Zhang, Z., Hu, X., Wang, G., Lin, Z., Wang, S., et al. (2013). mir-17-92 cluster is required for and sufficient to induce cardiomyocyte proliferation in postnatal and adult hearts. Circ. Res. *112*, 1557–1566.

Cornelissen, V.A., Vanhaecke, J., Aubert, A.E., and Fagard, R.H. (2012). Heart rate variability after heart transplantation: a 10-year longitudinal follow-up study. J. Cardiol. *59*, 220–224.

D'Uva, G., Aharonov, A., Lauriola, M., Kain, D., Yahalom-Ronen, Y., Carvalho, S., Weisinger, K., Bassat, E., Rajchman, D., Yifa, O., et al. (2015). ERBB2 triggers mammalian heart regeneration by promoting cardiomyocyte dedifferentiation and proliferation. Nat. Cell Biol. *17*, 627–638.

da Penha Berzaghi, M., Cooper, J., Castrén, E., Zafra, F., Sofroniew, M., Thoenen, H., and Lindholm, D. (1993). Cholinergic regulation of brain-derived neurotrophic factor (BDNF) and nerve growth factor (NGF) but not neurotrophin-3 (NT-3) mRNA levels in the developing rat hippocampus. J. Neurosci. *13*, 3818–3826.

Dhein, S., van Koppen, C.J., and Brodde, O.E. (2001). Muscarinic receptors in the mammalian heart. Pharmacol. Res. *44*, 161–182.

Drachman, D.B. (1964). Atrophy of skeletal muscle in chick embryos treated with botulinum toxin. Science *145*, 719–721.

Epstein, J.A., Aghajanian, H., and Singh, M.K. (2015). Semaphorin signaling in cardiovascular development. Cell Metab. *21*, 163–173.

Eulalio, A., Mano, M., Dal Ferro, M., Zentilin, L., Sinagra, G., Zacchigna, S., and Giacca, M. (2012). Functional screening identifies miRNAs inducing cardiac regeneration. Nature *492*, 376–381.

Gallego-Page, J.C., Segovia, J., Alonso-Pulpon, L., Alonso-Rodriguez, M., Salas, C., and Ortiz-Berrocal, J. (2004). Re-innervation after heart transplantation: a multidisciplinary study. J. Heart Lung Transplant. *23*, 674–682.

Gemberling, M., Karra, R., Dickson, A.L., and Poss, K.D. (2015). Nrg1 is an injury-induced cardiomyocyte mitogen for the endogenous heart regeneration program in zebrafish. eLife *4*, 4.

Godwin, J.W., Pinto, A.R., and Rosenthal, N.A. (2013). Macrophages are required for adult salamander limb regeneration. Proc. Natl. Acad. Sci. USA *110*, 9415–9420.

Heallen, T., Morikawa, Y., Leach, J., Tao, G., Willerson, J.T., Johnson, R.L., and Martin, J.F. (2013). Hippo signaling impedes adult heart regeneration. Development *140*, 4683–4690.

Huang, da W., Sherman, B.T., and Lempicki, R.A. (2009a). Bioinformatics enrichment tools: paths toward the comprehensive functional analysis of large gene lists. Nucleic Acids Res. *37*, 1–13.

Huang, da W., Sherman, B.T., and Lempicki, R.A. (2009b). Systematic and integrative analysis of large gene lists using DAVID bioinformatics resources. Nat. Protoc. *4*, 44–57.

Ieda, M., Kanazawa, H., Kimura, K., Hattori, F., Ieda, Y., Taniguchi, M., Lee, J.K., Matsumura, K., Tomita, Y., Miyoshi, S., et al. (2007). Sema3a maintains normal heart rhythm through sympathetic innervation patterning. Nat. Med. *13*, 604–612.

Jopling, C., Sleep, E., Raya, M., Martí, M., Raya, A., and Izpisúa Belmonte, J.C. (2010). Zebrafish heart regeneration occurs by cardiomyocyte dedifferentiation and proliferation. Nature *464*, 606–609.

Kikuchi, K., Holdway, J.E., Werdich, A.A., Anderson, R.M., Fang, Y., Egnaczyk, G.F., Evans, T., Macrae, C.A., Stainier, D.Y., and Poss, K.D. (2010). Primary contribution to zebrafish heart regeneration by gata4(+) cardiomyocytes. Nature *464*, 601–605.

Kikuchi, K., Holdway, J.E., Major, R.J., Blum, N., Dahn, R.D., Begemann, G., and Poss, K.D. (2011). Retinoic acid production by endocardium and epicardium is an injury response essential for zebrafish heart regeneration. Dev. Cell *20*, 397–404.

Kim, D., Pertea, G., Trapnell, C., Pimentel, H., Kelley, R., and Salzberg, S.L. (2013). TopHat2: accurate alignment of transcriptomes in the presence of insertions, deletions and gene fusions. Genome Biol. *14*, R36.

Kumar, A., and Brockes, J.P. (2012). Nerve dependence in tissue, organ, and appendage regeneration. Trends Neurosci. *35*, 691–699.

Kumar, A., Godwin, J.W., Gates, P.B., Garza-Garcia, A.A., and Brockes, J.P. (2007). Molecular basis for the nerve dependence of limb regeneration in an adult vertebrate. Science *318*, 772–777.

Laflamme, M.A., and Murry, C.E. (2011). Heart regeneration. Nature *473*, 326–335.

Lam, N.T., Currie, P.D., Lieschke, G.J., Rosenthal, N.A., and Kaye, D.M. (2012). Nerve growth factor stimulates cardiac regeneration via cardiomyocyte proliferation in experimental heart failure. PLoS ONE *7*, e53210.

Lapchak, P.A., Araujo, D.M., and Hefti, F. (1993). Cholinergic regulation of hippocampal brain-derived neurotrophic factor mRNA expression: evidence from lesion and chronic cholinergic drug treatment studies. Neuroscience *52*, 575–585.

Laube, F., Heister, M., Scholz, C., Borchardt, T., and Braun, T. (2006). Re-programming of newt cardiomyocytes is induced by tissue regeneration. J. Cell Sci. *119*, 4719–4729.

Lavine, K.J., Epelman, S., Uchida, K., Weber, K.J., Nichols, C.G., Schilling, J.D., Ornitz, D.M., Randolph, G.J., and Mann, D.L. (2014). Distinct macrophage lineages contribute to disparate patterns of cardiac recovery and remodeling in the neonatal and adult heart. Proc. Natl. Acad. Sci. USA *111*, 16029–16034.

Liao, R., and Jain, M. (2007). Isolation, culture, and functional analysis of adult mouse cardiomyocytes. Methods Mol. Med. *139*, 251–262.

Mahmoud, A.I., Kocabas, F., Muralidhar, S.A., Kimura, W., Koura, A.S., Thet, S., Porrello, E.R., and Sadek, H.A. (2013). Meis1 regulates postnatal cardiomyocyte cell cycle arrest. Nature *497*, 249–253.

Mahmoud, A.I., Porrello, E.R., Kimura, W., Olson, E.N., and Sadek, H.A. (2014). Surgical models for cardiac regeneration in neonatal mice. Nat. Protoc. *9*, 305–311.

Martelli, D., McKinley, M.J., and McAllen, R.M. (2014). The cholinergic anti-inflammatory pathway: a critical review. Auton. Neurosci. *182*, 65–69.

Meloni, M., Caporali, A., Graiani, G., Lagrasta, C., Katare, R., Van Linthout, S., Spillmann, F., Campesi, I., Madeddu, P., Quaini, F., and Emanueli, C. (2010). Nerve growth factor promotes cardiac repair following myocardial infarction. Circ. Res. *106*, 1275–1284.

Nam, J., Onitsuka, I., Hatch, J., Uchida, Y., Ray, S., Huang, S., Li, W., Zang, H., Ruiz-Lozano, P., and Mukouyama, Y.S. (2013). Coronary veins determine the pattern of sympathetic innervation in the developing heart. Development *140*, 1475–1485.

O'Meara, C., Wamstad, J.A., Gladstone, R., Fomovsky, G., Butty, V., Shrikumar, A., Gannon, J., Boyer, L., and Lee, R.T. (2015). Transcriptional reversion of cardiac myocyte fate during mammalian cardiac regeneration. Circ. Res. 116, 804–815.

Oberpriller, J.O., and Oberpriller, J.C. (1974). Response of the adult newt ventricle to injury. J. Exp. Zool. *187*, 249–253.

Pasumarthi, K.B., and Field, L.J. (2002). Cardiomyocyte cell cycle regulation. Circ. Res. *90*, 1044–1054.

Polizzotti, B.D., Ganapathy, B., Walsh, S., Choudhury, S., Ammanamanchi, N., Bennett, D.G., dos Remedios, C.G., Haubner, B.J., Penninger, J.M., and Kühn, B. (2015). Neuregulin stimulation of cardiomyocyte regeneration in mice and human myocardium reveals a therapeutic window. Sci. Transl. Med. *7*, 281ra45.

Porrello, E.R., Johnson, B.A., Aurora, A.B., Simpson, E., Nam, Y.J., Matkovich, S.J., Dorn, G.W., 2nd, van Rooij, E., and Olson, E.N. (2011a). MiR-15 family regulates postnatal mitotic arrest of cardiomyocytes. Circ. Res. *109*, 670–679.

Porrello, E.R., Mahmoud, A.I., Simpson, E., Hill, J.A., Richardson, J.A., Olson, E.N., and Sadek, H.A. (2011b). Transient regenerative potential of the neonatal mouse heart. Science *331*, 1078–1080.

Porrello, E.R., Mahmoud, A.I., Simpson, E., Johnson, B.A., Grinsfelder, D., Canseco, D., Mammen, P.P., Rothermel, B.A., Olson, E.N., and Sadek, H.A. (2013). Regulation of neonatal and adult mammalian heart regeneration by the miR-15 family. Proc. Natl. Acad. Sci. USA *110*, 187–192.

Poss, K.D., Wilson, L.G., and Keating, M.T. (2002). Heart regeneration in zebrafish. Science *298*, 2188–2190.

Puente, B.N., Kimura, W., Muralidhar, S.A., Moon, J., Amatruda, J.F., Phelps, K.L., Grinsfelder, D., Rothermel, B.A., Chen, R., Garcia, J.A., et al. (2014). The oxygen-rich postnatal environment induces cardiomyocyte cell-cycle arrest through DNA damage response. Cell *157*, 565–579.

Rottbauer, W., Saurin, A.J., Lickert, H., Shen, X., Burns, C.G., Wo, Z.G., Kemler, R., Kingston, R., Wu, C., and Fishman, M. (2002). Reptin and pontin antagonistically regulate heart growth in zebrafish embryos. Cell *111*, 661–672.

Saldanha, A.J. (2004). Java Treeview–extensible visualization of microarray data. Bioinformatics *20*, 3246–3248.

Singer, M. (1952). The influence of the nerve in regeneration of the amphibian extremity. Q. Rev. Biol. *27*, 169–200.

Singer, M., Davis, M.H., and Scheuing, M.R. (1960). The influence of atropine and other neuropharmacological substances on regeneration of the forelimb in the adult urodele, Triturus. J. Exp. Zool. *143*, 33–45.

Todd, J.T. (1823). On the process of reproduction of the members of the aquatic salamander. Quart. J. Sci. Lit. Arts *16*, 84–96.

Trapnell, C., Williams, B.A., Pertea, G., Mortazavi, A., Kwan, G., van Baren, M.J., Salzberg, S.L., Wold, B.J., and Pachter, L. (2010). Transcript assembly and quantification by RNA-Seq reveals unannotated transcripts and isoform switching during cell differentiation. Nat. Biotechnol. *28*, 511–515.

Tsonis, P.A., Madhavan, M., Tancous, E.E., and Del Rio-Tsonis, K. (2004). A newt's eye view of lens regeneration. Int. J. Dev. Biol. *48*, 975–980.

Xin, M., Kim, Y., Sutherland, L.B., Murakami, M., Qi, X., McAnally, J., Porrello, E.R., Mahmoud, A.I., Tan, W., Shelton, J.M., et al. (2013). Hippo pathway effector Yap promotes cardiac regeneration. Proc. Natl. Acad. Sci. USA *110*, 13839–13844.